

# A NEW APPROACH TO DESCRIBING THREE-DIMENSIONAL ORIENTATION DISTRIBUTION FUNCTIONS IN TEXTURED MATERIALS

## I. FORMATION OF POLE DENSITY DISTRIBUTION ON MODEL POLE FIGURES

V. N. DNIEPRENKO AND S. V. DIVINSKII

*Institute of Metal Physics, Ukrainian Academy of Sciences, Prospekt Vernadskogo  
36, Kiev-142, 252680, Ukraine*

New method for simulation of orientation distribution functions of textured materials has been proposed. The approach is based on the concept to describe any texture class by a superposition of anisotropic partial fibre components. The texture maximum spread is described in a "local" coordinate system connected with the texture component axis. A set of Eulerian angles  $\gamma_1, \gamma_2, \gamma_3$  are introduced with this aim. To specify crystallite orientations with respect to the sample coordinate system two additional sets of Eulerian angles are introduced besides  $\gamma_1, \gamma_2, \gamma_3$ . One of them,  $(\Psi_0, \theta_0, \Phi_0)$ , defines the direction of the texture axis of a component with respect to the directions of the cub. The other set,  $(\Psi_1, \theta_1, \Phi_1)$ , is determined by the orientation of the texture component and its texture axis in the sample coordinate system. Analytical expressions approximating real spreads of crystallites in three-dimensional orientation space have been found and their corresponding model pole figures have been derived. The proposed approach to the texture spread description permits to simulate a broad spectrum of real textures from single crystals to isotropic polycrystals with a high enough degree of correspondence.

KEY WORDS: Model ODF partial fibre components anisotropic spread orientation tubes.

## INTRODUCTION

The distribution of orientations in textured materials is known to be described by three-dimensional functions  $f(g_B)$ , with the crystallite orientations  $g_B$  being commonly specified by three Eulerian angles  $\phi_1, \Phi$  and  $\phi_2$ , see Bunge (1969). The most widely used method for finding the texture, i.e. the predominant orientations of grains in a specimen, is plotting the pole figures (PF) from diffraction measurement data. In this case the Orientation Distribution Functions (ODF) are found with the use of mathematical techniques of texture analysis. Most often the coefficients of the ODF expansion into a series in terms of generalized spherical functions are computed and charts of ODF sections in the space of the angles  $(\phi_1, \Phi, \phi_2)$  are plotted, Bunge(1969), Roe (1965). In addition to the arising difficulties associated with the truncation of the series only even coefficients of the expansion may be obtained directly. This results in false maxima and negative values of the ODF (if no ghost correction is used).

The errors of ODF reconstruction from pole figures cause development of new methods for its solution by means of some additional information about the ODF

structure. In this case the ODF approximations by some model functions (mainly by the Gaussian-type ones) are used, see Bunge (1969), Jura (1988), Savelova (1984), Matthies (1982), Lucke, Pospiech, Virnich, Jura (1981).

There are three different approaches to describe the real rolling textures by model functions. In one of them the texture is described by a system of preferred orientations. In this case the so-called "spherical" distributions describing an isotropic spread of pole density with respect to maxima of such preferred orientations are used by Bunge (1969), Matthies (1982), Savelova (1984) and other. For improving the agreement between theory and experiment the extra texture components occupying an intermediate positions between the main ones are to be introduced in such approaches. For example, for the so-called standard distribution of the Gaussian type suggested by Matthies (1982), the corresponding pole density  $P_{(\bar{h})}$  on PF  $\bar{h}$  has the form

$$P_{(\bar{h})}(g_B^0, b, \bar{y}) = P_{(\bar{h})}(S, z) = \exp\{S(z-1)/2\} \frac{I_0(S(z+1)/2)}{I_0(S) - I_1(S)}, \quad (1)$$

where  $g_B = (\varphi_1, \Phi, \varphi_2)$  is the position of the maximum in the Eulerian angle space;  $S$  is the spread parameter determined by a width  $b$  at half maximum;  $\bar{y} = (\alpha, \beta)$  are the spherical coordinates of a point on the PF;  $z = \bar{h} \cdot g_B^0 \cdot \bar{y}$ ; and  $I_n(x)$  are the modified Bessel's functions. From this expression it is seen that the pole density spread as well that of the ODF are isotropic, i.e., they are described by a single parameter  $b$  (or  $S$ ). This is valid for all the model ODF's suggested up to now. Savelova (1984) suggested a function to describe anisotropic spread of orientation maxima on the  $SO(3)$  rotational group but this has been done without any connection to real ODFs. From our point of view, the difficulties in her approach are connected with disregarding the texture axis concept and thus the necessity to consider a tensor character of orientation spread  $\varepsilon_{ij}\beta_i\beta_j$  by Eulerian angles  $\beta_1, \beta_2, \beta_3$ .

Some rolling textures especially of b.c.c. metals have been presented by Jura (1988) as a superposition of fibre components and spherical distributions around to preferred orientation maxima.

The third approach has been proposed by Wassermann, Grewen (1962) about thirty years ago. It consists in a description of rolling textures of both f.c.c. and b.c.c. metals by a superposition of partial fibre components. In this case texture axes, i.e. rotations axes relative to which the component spreads are conditionally formed, can be selected. In this case pole density depends on a turning angle around such axes unlike fibre textures for which the pole density is constant under rotations around the fibre axis.

For rolling textures the pole density distribution with respect to the maxima is known to differ from isotropic in general case, see Wassermann *et al.* (1962). Hence the introduction of several spread parameters into the model ODF is needed.

The principle of the ODF rolling texture simulation for both f.c.c. and b.c.c. metals by a superposition of the partial fibre components is given in this paper. A model distribution function allows to introduce a spread anisotropy relative to the preferred orientations.

## THEORY

We confine our analysis to most typical textures: "ideal orientations" with spherical spread (isotropic with respect to distribution maxima), fibre, and partial fibre ones.

The description by the “ideal-orientations” can be applicable to recrystallized metals. Fibre textures are formed after axially-symmetrical external actions. Rolling textures are mostly a superposition of partial fibre components. For example, basing on ideas of Wassermann *et al.* (1962), the rolling texture of  $\alpha$ -Fe can be described by a sum of two partial fibre components – see Figure 1a) – d). The texture axes are indicated

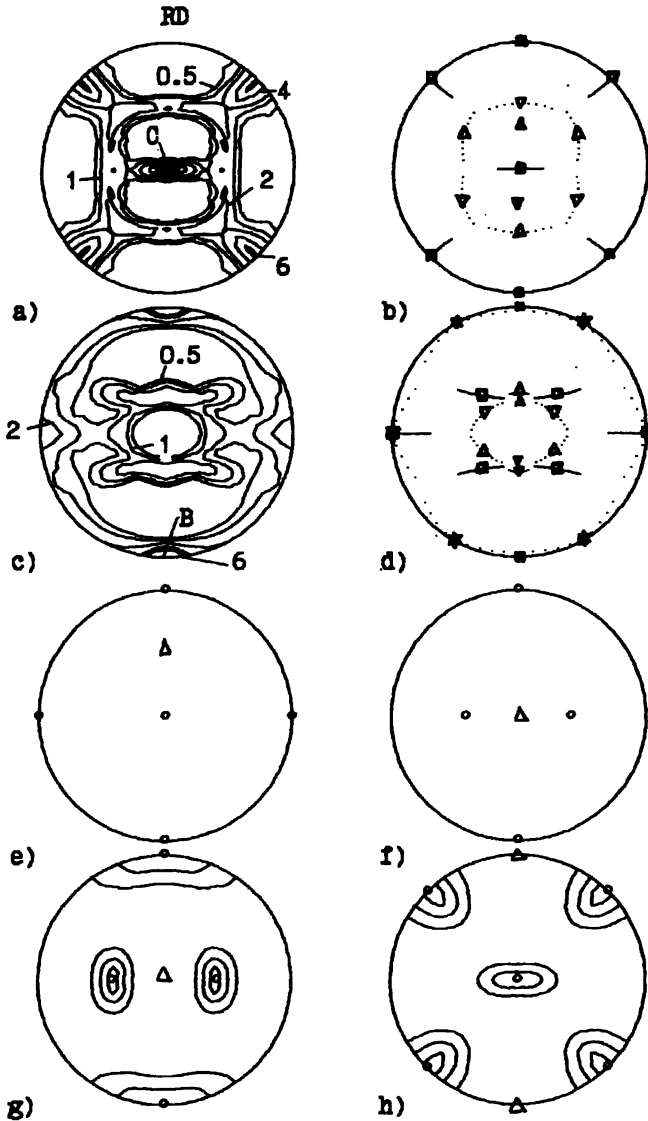


**Figure 1** Experimental pole figures {200} (a) and {110} (c) of  $\alpha$ -Fe rolling texture with the diagram of their formation on the basis of a superposition of three partial fibre components (b,d): — □ — (001)[110], ■ its axis; · · △ · · (111)[112], ▲ its axis; · · ▽ · · (111)[112], ▼ its axis. B and C are maxima from which the texture component parameters were determined. Formation of (001)[110] texture component is presented schematically by a sequence e) – h).

by special symbols. The presence of anomaly high maxima of pole density on some experimental PFs may be explained by the existence of texture components that can be characterized as partial fibre ones. In present meaning an "anomaly high" maximum is a maximum with intensity several times greater than that of other maxima of the same component. Especially for PFs with indices  $\{hkl\}$  close to crystallographic axis of partial fibre component the existence of such "anomaly high" maxima is most pronounced. This arises from the fact that as the distance to the texture axis decreases the pole density increases sharply. For fibre textures this is most obvious. But up to now Wassermann's model remains a qualitative one and takes no account for real spread of pole density on PFs. Also it does not say anything about the crystallite distribution on orientation i.e. about ODF of the sample.

For the model ODF it appears to be more natural if it will be based on features of the texture symmetry and will not be referred to arbitrarily selected coordinate directions of the sample. Due to this, we will describe the crystallite spread of  $i$ -th component relative to a coordinate system  $K_i$  connected with the texture axis of this component. It should be noted that the description of crystallite spread with respect to the external sample coordinate system  $K_s$  is traditionally adopted in texture analysis.

Let the  $Oz$ -axis of the component coordinate system  $K_i$  coincides with the direction of its texture axis. Usually the orientation of a particular crystallite is defined by a set of three Eulerian angles which are necessary to rotate the crystallite coordinate system  $K_0$  with the coordinate directions being along directions of the cube to the sample coordinate system  $K_s$ . Now the following sets of rotations are introduced to describe the crystallite orientation:

- $(\Psi_0^{(i)}, \theta_0^{(i)}, \varphi_0^{(i)})$ , that aligns  $K_0$  with the component coordinate system  $K_i$ . Note that the texture axis of the  $i$ -th component coincides with the  $Oz$ -axis of the current coordinate system;
- $(\gamma_1, \gamma_2, \gamma_3)$ , designates rotations which specify the spread of the crystallite orientation with respect to the texture axis. Now  $K_0$  has been rotated relative to  $K_i$  by  $\gamma_1, \gamma_2, \gamma_3$ ; and
- $(\Psi_1^{(i)}, \theta_1^{(i)}, \varphi_1^{(i)})$ , which turns  $K_i$  to the final position characterized by the  $(hkl)[uvw]$  orientation required. At this  $K_0$  becomes coincident with  $K_s$ . Thus, we characterize the crystallite orientation by its spread relatively to the component texture axis instead with respect to the sample coordinate system.

Any set of three angles in this paper determines the following sequence of rotations: the coordinate system is first rotated around the  $Oz$ -axis, then around the new direction of the  $Ox$ -axis, and finally once again around the  $Oz$ -axis in its final position.

Now modelling of a texture component can be presented schematically by Figure 1 e) – h). In this figure, e) presents the stereographic projection of an initial single crystal; f) is the same after rotations by  $\Psi_0, \theta_0, \varphi_0$  which aligns the texture axis  $\Delta$  parallel to  $Oz$ ; g) shows the grain spread formed in the polycrystal by rotations  $\gamma_1, \gamma_2, \gamma_3$ ; h) is the final position after the rotation  $\Psi_1, \theta_1, \varphi_1$ . These diagrams correspond to the sequence of simulation of the  $\{001\}\langle 110 \rangle$  component of typical b.c.c. metals rolling texture.

It can be assumed that the description of the crystallite orientation spread with respect to the selected texture axis of a component with coordinates  $(\gamma_1, \gamma_2, \gamma_3)$  will be simpler than for  $(\varphi_1, \Phi, \varphi_2)$  introduced by Bunge.

Let us find the relation between the sets of angles  $g_B = (\varphi_1, \Phi, \varphi_2)$  and  $G = (\Psi_0, \theta_0, \varphi_0, \gamma_1, \gamma_2, \gamma_3, \Psi_1, \theta_1, \varphi_1)$ . From the construction of  $G$  it is clear that

$$G = g_0 \cdot g_\gamma \cdot g_1, \tag{2}$$

where  $g_0, g_\gamma, g_1$  are matrices of rotations corresponding to the angle sets  $(\Psi_0, \theta_0, \phi_0)$ ,  $(\gamma_1, \gamma_2, \gamma_3)$  and  $(\Psi_1, \theta_1, \phi_1)$ , respectively. Equating the proper elements of  $g_B$  and  $G$  and solving the trigonometric equations we obtain relations of the form

$$\begin{cases} \varphi_1 = \varphi_1(\Psi_0, \theta_0, \phi_0, \gamma_1, \gamma_2, \gamma_3, \Psi_1, \theta_1, \phi_1) \\ \Phi_1 = \Phi_1(\Psi_0, \theta_0, \phi_0, \gamma_1, \gamma_2, \gamma_3, \Psi_1, \theta_1, \phi_1) \\ \varphi_2 = \varphi_2(\Psi_0, \theta_0, \phi_0, \gamma_1, \gamma_2, \gamma_3, \Psi_1, \theta_1, \phi_1) \end{cases} \tag{3}$$

The general form of the relations is too cumbersome to present them here. They will be further given for some particular cases.

To find an analytical form of the ODF  $f(G)$  in dependence on the set of angles  $g_\gamma = (\gamma_1, \gamma_2, \gamma_3)$  describing the spread we will do in the following manner. Firstly let us consider a recrystallization texture of f.c.c. metals. Its approximation as a function of angles  $g_B = (\varphi_1, \Phi, \varphi_2)$  is very simple, see Lucke *et al.* (1981). Next,  $f(G)$  may be derived by using formula (3). After words we generalized the obtained results to the case of rolling texture. It is necessary to note that the recrystallization textures are not studied in the present work. They are used only for construction of the model functions. Sections of the ODF for copper recrystallization texture are shown for  $\varphi_1 = const$  planes in Figure 2. The ODF has been reconstructed from the {200}, {110}, {222} pole figures by series expansion with even terms. Because of the small value of texture spread we

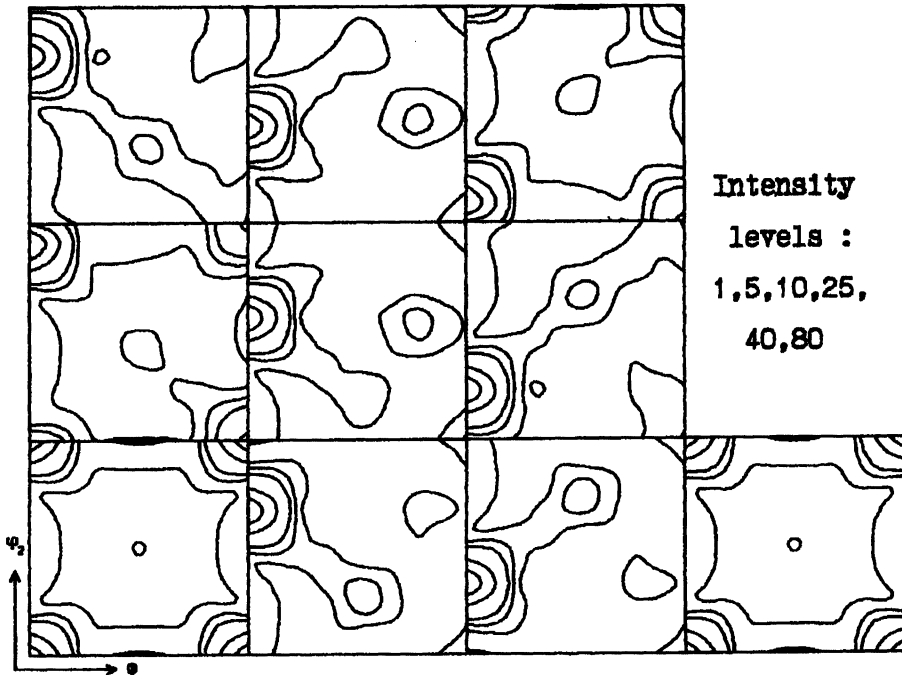


Figure 2 The ODF  $f(g_B)$  of the cube texture of recrystallized Cu.

may write approximation formulas instead using Matthies's standard functions (Matthies, 1982). It is convenient to do this separately for each ODF maximum, since the own set of rotations  $g_0$  and  $g_1$  corresponds to each maximum. It should be noted that some maxima of the ODF in Figure 2 are ghosts, i.e. they do not represent true maxima in the orientation distribution as well as in Lucke *et al.* (1981). Therefore we will consider the cube orientations only. Thus for a spread around the preferred orientation of such types as  $(\varphi_1^0, \pi/2, \varphi_2^0)$ , where  $\varphi_1^0, \varphi_2^0$  take the values of 0,  $\pi/2$ , we have

$$f(\varphi_1, \Phi, \varphi_2) \sim \exp \left\{ - \frac{(\Phi - \pi/2)^2 + (\varphi_1 - \varphi_1^0)^2 + (\varphi_2 - \varphi_2^0)^2}{2 \sigma^2} \right\}, \quad (4)$$

with  $\sigma \cong 0.16$ .

In turn for preferred orientations of such types as  $\Phi^0=0, \varphi_1^0+\varphi_2^0=0, \pi/2, \pi$  the ODF spread is described by

$$f(\varphi_1, \Phi, \varphi_2) \sim \exp \left\{ - \frac{\Phi^2 + (\varphi_1 + \varphi_2 - (\varphi_1^0 + \varphi_2^0))^2}{2 \sigma^2} \right\}. \quad (5)$$

Here we considered only the case of a spherical ODF spread with respect to the maxima. The possibility of an asymmetrical spread of texture maxima relative to preferred orientations was long ago pointed out by Wassermann *et al.* (1962). Let us consider the ODF for a hypothetical cube texture with an asymmetrical spread of maxima. The asymmetry was introduced directly into the pole density distribution "by hand" following Wassermann's ideas and considering the normal direction in the PFs as the direction of the texture axis. In Figure 3b the PF's {100}, {110}, and {111} obtained in such way are shown. This texture is described by the preferred (001)[100] orientation with the [001] texture axis. The radial and the azimuthal dispersions were taken at 0.10 and 0.24, respectively. Here and afterwards the radial angle is counted off from the texture axis while the azimuthal one determines a rotation around this axis. The calculated ODF is presented in Figure 3a. The texture spread is now approximated by Gaussian distributions of the form

$$f(\varphi_1, \Phi, \varphi_2) \sim \exp \left\{ - \frac{(\Phi - \pi/2)^2 + (\varphi_2 - \varphi_2^0)^2}{2 \sigma_1^2} \right\} \exp \left\{ - \frac{(\varphi_1 - \varphi_1^0)^2}{2 \sigma_2^2} \right\},$$

for  $g_B^0 = (\varphi_1^0, \pi/2, \varphi_2^0), \varphi_1^0, \varphi_2^0 = 0, \pi/2$ ; (6)

$$f(\varphi_1, \Phi, \varphi_2) \sim \exp \left\{ - \frac{\Phi^2}{2 \sigma_1^2} \right\} \exp \left\{ - \frac{(\varphi_1 + \varphi_2 - (\varphi_1^0 + \varphi_2^0))^2}{2 \sigma_2^2} \right\},$$

for  $g_B^0 = (\varphi_1^0, 0, \varphi_2^0), \varphi_1^0 + \varphi_2^0 = 0, \pi/2, \pi$ .

Let us consider these maxima on the basis of the concept of partial fibre textures. The texture symmetry results in that the ODF has  $N$  maxima with the coordinates  $g_{B_i}^0, i = 1, \dots, N$ , each of which corresponds to some preferred orientations of the  $\{hkl\} \langle uvw \rangle$

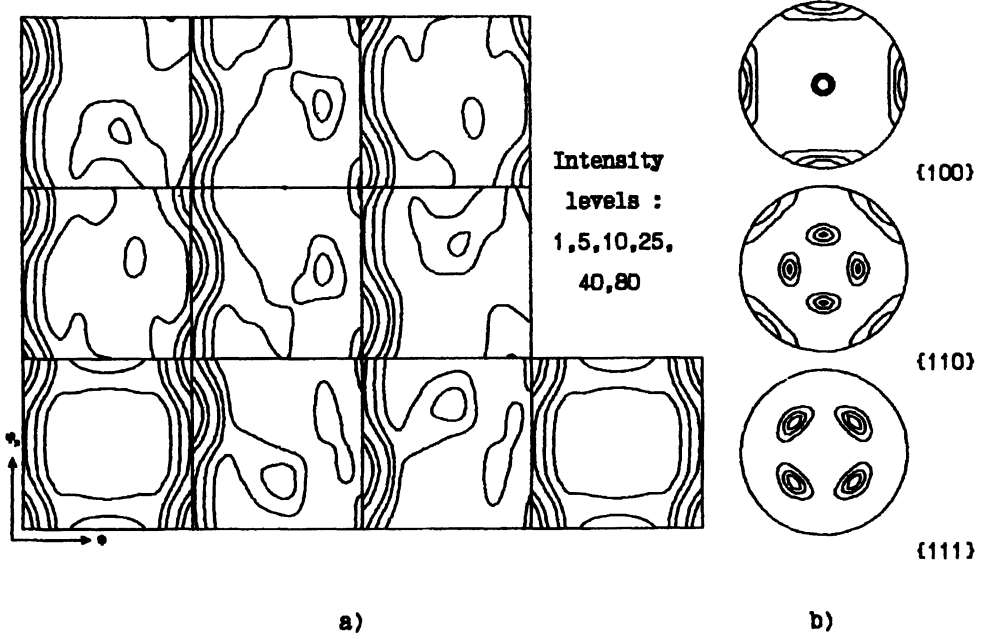


**Figure 3** The ODF (a) and the theoretical pole figures (b) for (001)[100] texture with an asymmetrical spread of maxima.

family. The position of the  $[u'v'w']$  texture axis is determined by external conditions of the formation of the texture itself. Both for the rolling case (Figure 1a,c) and for the case presented in Figure 3 the texture axes make certain angles with the external characteristic directions (or with  $(hkl)$  and  $[uvw]$ ). Consequently a specific crystallographic direction from the  $\langle u'v'w' \rangle$  family is the texture axis of every specific preferred  $(hkl)[uvw]$  orientation which is presented by a maximum in the space of angles  $g_B = (\varphi_1, \Phi, \varphi_2)$ . Thus, the specific values of rotations  $g_{0i} = (\Psi_{0i}, \theta_{0i}, \varphi_{0i})$  and  $g_{1i} = (\Psi_{1i}, \theta_{1i}, \varphi_{1i})$  determined earlier will correspond to every texture maximum  $g_{B_i}^0$ . Let us consider each maximum  $g_{B_i}^0$  separately. For the texture maximum  $g_B^0 = (\pi/2, \pi/2, \pi/2)$  corresponding to (100)[001] preferred orientation with texture axis [100] (Figure 3) we have

$$g_0 = \begin{vmatrix} 0 & 0 & 1 \\ 0 & -1 & 0 \\ 1 & 0 & 0 \end{vmatrix}, \quad g_1 = \begin{vmatrix} 1 & 0 & 0 \\ 0 & 1 & 0 \\ 0 & 0 & 1 \end{vmatrix} \quad (7)$$

and formulas (3) change to

$$\begin{cases} \cos\Phi = \sin\gamma_3 \sin\gamma_2 \\ \cos\varphi_1 \sin\Phi = -\sin\gamma_1 \cos\gamma_3 - \cos\gamma_1 \sin\gamma_3 \cos\gamma_2 \\ \cos\varphi_2 \sin\Phi = -\cos\gamma_3 \sin\gamma_2 \end{cases} \quad (8)$$

Considering small derivations from the preferred orientation we can write:

$$\begin{cases} \Phi - \pi/2 \approx 0 \\ \varphi_1 - \pi/2 \approx -\gamma_1 - \gamma_3 \\ \varphi_2 - \pi/2 \approx -\gamma_2 \end{cases} \quad (9)$$

Let us consider in such way all maximum (6). The following common expression for  $f(\gamma_1, \gamma_2, \gamma_3)$  under the condition  $\sigma_1, \sigma_2 \ll \pi/2$  may be written:

$$f^M(\gamma_1, \gamma_2, \gamma_3) \sim \exp\left\{-\frac{\gamma_2^2}{2\sigma_1^2}\right\} \exp\left\{-\frac{(\gamma_1 + \gamma_3)^2}{2\sigma_2^2}\right\} \quad (10)$$

For "ideal" textures (5) where the spread on the PF's relative to the maxima is isotropic the ODF is described by expression (10) with  $\sigma_1 = \sigma_2$ . In this case any conventional position of the texture axis may be selected because of the equality of the radial and the azimuthal spread.

## PRINCIPLE OF CONSTRUCTION OF THEORETICAL POLE FIGURES

We have discussed the simplest cube texture or a hypothetical (001)[100] texture with a non spherical spread of the ODF maxima. Assume that the result (6)–(10) is a common one, i.e. any partial fibre component (hkl)[uvw] with an axis [u'v'w'] can be described in the space of angles  $G$  by a function (10).

We will demonstrate this by the way of PF calculation. Let us determine the pole density distribution  $P_{(\bar{h})\bar{y}}$  on the PF  $\bar{h}$  for the above-adopted model ODF. The unit vector  $\bar{y}$  is given by the spherical coordinates of a direction on the PF.

Let us introduce an angle  $\delta$  determining the rotation of the crystallite around an axis coinciding with  $\bar{h}_i$ , when  $\bar{h}_i \parallel \bar{y}$ ;  $\bar{h}_i \cdot \bar{y} = 1, \dots, M$  are equivalent planes from the  $\{\bar{h}\}$  family. The  $\delta$  value (together with  $\bar{h}$ ) also determines uniquely the orientation of the crystallite.

In the general case the pole density distribution  $P_{(\bar{h})\bar{y}}$  may be obtained as follows:

$$P_{(\bar{h})}(\bar{y}) = \sum_{i=1}^M \sum_{k=1}^N \frac{p_k}{2\pi M} \int_0^{2\pi} f^M(\gamma_1^{(ik)}, \gamma_2^{(ik)}, \gamma_3^{(ik)}) d\delta, \quad (11)$$

where

$$g_{\bar{y}}^{(ik)} = [g_0^{(k)}]^{-1} \cdot g_B^{(i)} \cdot \Omega(\delta) \cdot [g_1^{(k)}]^{-1} \quad (11a)$$

Here  $g_B^{(i)}$  is the matrix of rotation for the crystallite orientation with  $\bar{y} = \bar{h}_i$ ,  $g_B^{(i)}$  in other words, the direction of  $\bar{h}_i$  is parallel to  $\bar{y}$  after rotation by  $g_B^{(i)} = (\varphi_1^{(i)}, \Phi^{(i)}, \varphi_2^{(i)})$ ;  $\Omega(\delta)$  is the matrix of rotations with the angle  $\delta$  defined above; the matrices  $g_0^{(k)}$  and  $g_1^{(k)}$  define a coordinate system connected with the axis of the texture component number  $k$ ,  $k = 1, \dots, N$ ;  $g_{\bar{y}}^{(ik)}$  is the matrix of rotations by the Eulerian angles  $\gamma_1^{(ik)}$ ,  $\gamma_2^{(ik)}$  and  $\gamma_3^{(ik)}$ ;  $p_k$  are the volume fractions of the texture components and  $\sum_{k=1}^N p_k = 1$ .

In this manner the model PFs, which correspond to the cube texture and to the hypothetical ones shown in Figure 3, may be easily obtained.

### DESCRIPTION OF ORIENTATION TUBES

A function of the type (10) allows to simulate adequately a great number of experimental textures. However for a successful simulation of real rolling textures the texture spreads in so-called orientation tubes analyzed by Hirsch, Lucke (1988) should be described. As it was shown by Hirsch *et al.* (1988), in this case the values of the ODF  $f(g_B)$  remain almost unchanged over the entire length of the orientation tube. Jura (1988) has proposed the use of axial components to describe such texture spreads. As we have considered, the use of the concept of partial fibre components is more naturally. In this case a functional dependence of  $f^M$  upon  $\gamma_1 + \gamma_3$  of the following type

$$f^M \sim \begin{cases} 1, & |\gamma_1 + \gamma_3| \leq \sigma_3 \\ \exp\left\{-\frac{1}{2} \left(\frac{|\gamma_1 + \gamma_3| - \sigma_3}{\sigma_2}\right)^2\right\}, & |\gamma_1 + \gamma_3| > \sigma_3 \end{cases} \quad (12)$$

can be introduced in formula (10) to describe such texture spreads. As can be seen from (12) the parameter  $\sigma_3$  characterizes the length of the region with a constant density of orientations in the orientation space, while  $\sigma_2$  determines the character of decrease of the density at the edges of the resulting orientation tube. Formula (12) is suitable for ODF simulation since with  $\sigma_3 = 0$  it results in a Gaussian spread around a preferred orientation and coincides with the previously proposed formula (10). In the latter case  $\sigma_2$  in (10) and (12) are simply identical. The model ODF  $f^M(G)$  will take the following form:

$$f^M(\gamma_1, \gamma_2, \gamma_3) = A \exp\left\{-\frac{\gamma_2^2}{2\sigma_1^2}\right\} \times \exp\left\{-\frac{1}{2} \left(\frac{|\gamma_1 + \gamma_3| - \sigma_3 + |\sigma_3 - |\gamma_1 + \gamma_3||}{2\sigma_2}\right)^2\right\}. \quad (13)$$

A is the normalization factor for the model ODF.

### FACTORS EFFECTING THE DISTRIBUTION OF POLE DENSITY ON THE MODEL PF

To simulate adequately real PFs the pole density distribution corresponding to the model ODF (13) should be calculate. Let us examine the spread variation for the angles  $\alpha$  and  $\beta$  in dependence on the parameters  $\sigma_1; \sigma_2; \sigma_3$  for various reflexes  $\bar{h}_i = (\alpha_0, \beta_0)$  with

different  $\alpha_0$  and  $\beta_0$ . The angles  $\alpha$ ,  $\beta$ ,  $\alpha_0$ , and  $\beta_0$  are determined in the coordinate system where the spread is formed. The angles  $\alpha_0$  and  $\alpha$  are the radial ones, i.e. the angles between the  $Oz$ -axis and the direction of  $\bar{h}$  or  $\bar{y}$ ;  $\beta_0$  and  $\beta$  are the azimuthal angles, i.e. the angles between the  $Ox$ -axis and the projection of directions  $\bar{h}$  or  $\bar{y}$  on the  $Oxy$  plane. In other words, we will perform the rotation  $g_0$  and  $g_r$ . Rotations  $g_1$  will not change the character of the spread but will only transfer the representation into a new coordination system.

The analysis demonstrates that a spherical Gaussian distribution is obtained on the PFs for  $\sigma_1 = \sigma_2$ ,  $\sigma_3 = 0$ . In this case the integral volumes of maxima with different  $\alpha_0$  coincide although the parameters of spread in  $\alpha$  and  $\beta$  ( $\sigma_\alpha$  and  $\sigma_\beta$  respectively) are not equal one to another for all  $\alpha_0 \neq \pi/2$ . This is caused by the fact that the parameters  $\sigma_\alpha$  and  $\sigma_\beta$  are related by  $\sigma_\beta \equiv \sigma_\alpha / \sin(\alpha_0)$ . All the maxima are equivalent in as far as they may be transformed one into another by corresponding rotations  $g_1$ . The height of the peaks does not depend on their positions on the PF (or coordinates  $\alpha_0$  and  $\beta_0$ ).

If  $\sigma_2$  increases ( $\sigma_2 > \sigma_1$  and  $\sigma_3 = 0$ ) or  $\sigma_3$  becomes non-zero, the relation between the heights of the maxima with various  $\alpha_0$  changes and the profiles of distribution in  $\alpha$  become asymmetrical. The asymmetry and height increase as a maximum approaches the textures axis. However the half-width of the pole density spread on the PF's in  $\alpha$  depends slightly on  $\sigma_2$  and  $\alpha_0$ , and coincides accurately enough with that of the ODF  $f(G)$  in angle  $\gamma_2$ . The latter can be used for determination of  $\sigma_1$  from experimental PFs.

The distributions in  $\beta$  at  $\alpha_0 = \pi/2$  for all  $\sigma_2 \neq 0$  and  $\sigma_3 = 0$  are Gaussian with dispersion  $\sigma = \sigma_2$ . The pattern is more complex at  $\sigma_0 \neq \pi/2$ . As has been noted for the case of  $\sigma_1 = \sigma_2$  we have  $\sigma_\beta > \sigma_\alpha = \sigma_1 = \sigma_2$ . If  $\sigma_2$  becomes greater than  $\sigma_1$ , the difference between  $\sigma_\beta$  and  $\sigma_2$  diminishes and becomes almost insignificant at  $\sigma_2 \geq 3\sigma_1$ . This is also valid for  $\sigma_3 + \sigma_2 \geq 3\sigma_1$  when  $\sigma_3 \neq 0$ . In this case the combination of parameters  $\sigma_2 + \sigma_3$  for the model ODF can be estimated directly from experimental PF's. The length of the region with a constant pole density may determine the  $\sigma_3$ . However it should be noted that in most cases this method may not be applicable due to the overlapping "tails" of the spreads of maxima with different  $\alpha_0$  and  $\beta_0$ . Therefore another method will be proposed below.

The spread of the maximum corresponding to the texture axis (i.e.  $\alpha_0 = 0$ ) is a spherical Gaussian one with dispersion  $\sigma = \sigma_1$  at any values of  $\sigma_2$  and  $\sigma_3$ . This fact directly follows from relations (11), (11a). In the coordinate system connected with the texture axis (11a) transforms into  $g_r = g_B \cdot \Omega(\delta)$ , i.e.  $\gamma_1 = \beta - \pi/2$ ,  $\gamma_2 = \alpha$ , and  $\gamma_3 = \delta$ . The constant term  $\beta - \pi/2$  in  $\gamma_1 + \gamma_3$  can be neglected under integration with respect to  $\delta$  over the full period  $2\pi$ . Then dropping the contributions of maxima with  $\alpha_0 \neq 0$  to the pole density near the texture axis we obtain for the texture axis

$$\begin{aligned}
 P_{(\bar{h})}(\alpha, \beta) &= \frac{A}{2\pi M} \int_0^{2\pi} \exp\left\{-\frac{\alpha^2}{2\sigma_1^2}\right\} \exp\left\{-\frac{1}{2} \frac{(\delta - \sigma_3 + |\sigma_3 - \delta|)^2}{4\sigma_2^2}\right\} d\delta = \\
 &= \frac{A \cdot I}{2\pi M} \exp\left\{-\frac{\alpha^2}{2\sigma_1^2}\right\}, \quad (14)
 \end{aligned}$$

where  $I$  is the normalization factor. The following relation for the ratio of pole densities of the maxima with  $\alpha_0 = 0$  ( $I_0$ ) and  $\alpha_0 \neq 0$  ( $I_{\alpha_0}$ ) can be obtained for  $\sigma_1, \sigma_2, \sigma_3 \ll \pi$ :

$$I_0/I_{\alpha_0} \cong \sqrt{\sin^2 \alpha_0 ((\sigma_2 + \sigma_3) / \sigma_0)^2 + \cos^2 \alpha_0}. \quad (15)$$

Basing on relation (15)  $\sigma_2 + \sigma_3$  can be estimated with known  $\sigma_1$  and  $I_0/I_{\alpha_0}$ .

## CONSTRUCTING MODEL POLE FIGURES FROM EXPERIMENTAL DATA

Employing the results presented above it is possible to construct model distributions of the pole density corresponding to experimental textures, i.e. to determine the ODF of the material in an analytical form. Let us consider the  $\alpha$ -Fe rolling texture. Experimental PFs are presented in Figure 1.a,c. This rolling texture may be described by a sum of partial fibre components (001)[110] and two symmetrical ones (111)[ $\bar{1}\bar{1}2$ ] and (111)[11 $\bar{2}$ ] with the texture axes near [110] (see Figure 1.a-d). The parameters of spread of the main partial fibre component (001)[110] with the texture axis [110] will be determined firstly. The  $\sigma_1$  value can be estimated as follows. Consider the maximum at the centre of the PF {200} or the maximum coinciding with RD on PF {110}. Gaussian approximation of spread of the selected maximum on PF {200} along the line connecting the PF centre with RD gives  $\sigma_1 = 0.07$ . The same value is obtained by approximation of the maximum B on PF {110}. From the relation of intensities of maxima B and C we obtain  $\sigma_2 + \sigma_3 = 0.34$  using formula (15) with  $\alpha_0 = \pi/2$ . From PF {200} (Figure 1.a) we get  $\sigma_3 = 0.12$  by analyzing the length of the region with a constant pole density along the line from the PF centre to the transversal direction (TD).

Next, using the analytical form of the ODF (10) we calculate  $P_{\{h\}}(\bar{y})$  at  $h$  {200} and {110} for the (001)[110] component with the texture axis [110] and subtract them from the initial experimental ones. For this it is necessary to renormalize the pole density  $P_{\{h\}}^m(\bar{y})$  of the component (001)[110] according to the expression

$$P_{\{h\}}^r(\bar{y}) = P_{\{h\}}^m(\bar{y}) \cdot \frac{P_B}{P_B^m}, \quad (16)$$

where  $P_{\{h\}}^r(\bar{y})$  is the renormalized pole density,  $P_B$  is the intensity in the point B of experimental PF {110} – Figure 1.b,  $P_B^m$  is the pole density for a model component in the same point. Analysis shows that the remaining pole density distribution is the sum of two symmetrical components (111)[ $\bar{1}\bar{1}2$ ] and (111)[11 $\bar{2}$ ] with the texture axis [221] (Figure 4). In this case  $\sigma_1$  is determined from the approximation of maximum A (Figure 4.b), but  $\sigma_2 + \sigma_3$  does from a relation of the intensities in maxima A and B (Figure 4b). We find  $\sigma_1 = 0.08$  and  $\sigma_2 + \sigma_3 = 0.49$ . More thorough analysis gives  $\sigma_2 = 0.05$ ,  $\sigma_3 = 0.44$ .

It should be noted that the texture axis [110] is hypothetically pointed out for the partial fibre component  $\{111\}\langle 11\bar{2} \rangle$  in the Wassermann model (Wassermann *et al.* (1962)) and in the experimental work of Schläfer, Bunge (1974). Analysis by means of model PFs and ODF sections shows that the positions of partial fibre component axes effect the PFs substantially more than the ODFs. Therefore the comparison of experimental PFs with model ones is to prefer for a reliable determination of the texture axes. Strong differences from experiment are observed in a case of the [110] axis for the (111)[11 $\bar{2}$ ] partial fibre component in the model PFs, especially for the {100} pole figure, see Figure 5c.

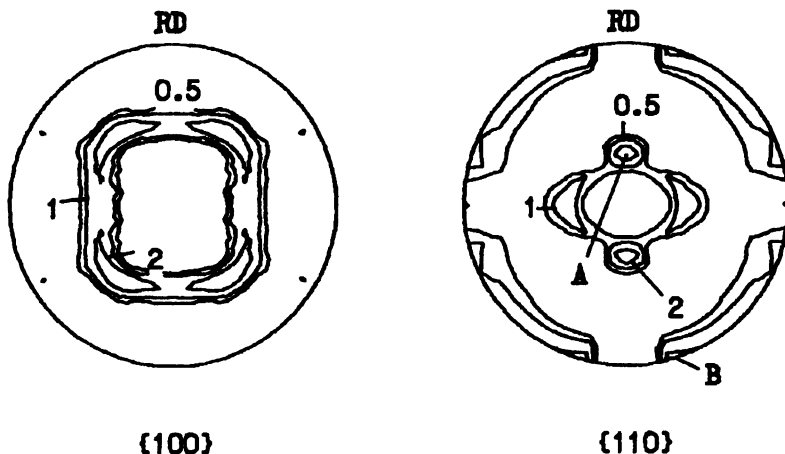


**Figure 4** The pole figures  $\{200\}$  and  $\{110\}$  which were obtained from Figure 1a, b by subtracting the pole density for the  $(001)[100]$  component with  $[110]$  texture axis. The model parameters of the component are:  $\sigma_1 = 0.07$ ,  $\sigma_2 = 0.22$ ,  $\sigma_3 = 0.12$ .

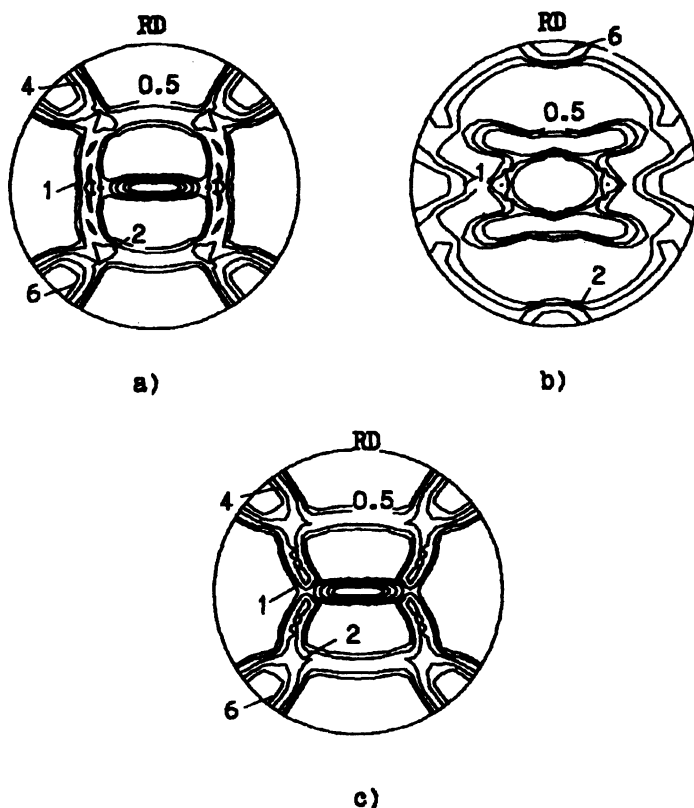


**Figure 5** The model pole figures  $\{100\}$  (a) and  $\{110\}$  (b) for  $\alpha$ -Fe rolling texture and  $\{100\}$  one for the case of  $[110]$  texture axis for  $(111)[112]$  partial fibre component (c).

Thus, all distribution parameters are estimated from experimental PFs to simulate the ODF by superposition of partial fibre components. The resulting model PFs {100} and {110} are shown in Figure 5a,b. In this case the experimental pole density  $P_{\{\bar{h}\}}^e(\bar{y})$  in Figure 1a,c can be given as a sum of model components

$$P_{\{\bar{h}\}}^e(\bar{y}) \approx \sum_{k=1}^3 V_k P_{\{\bar{h}\}}^{(k)}(\bar{y}) . \quad (17)$$

$V_k$  presents the volume fractions of various components contained in the initial texture. It should be noted that the values of  $P_{\{\bar{h}\}}^{(k)}(\bar{y})$  have to be normalized for correct use of expression (17).

Therefore, in the case under consideration the  $\alpha$ -Fe rolling texture contains  $\sim 70\%$  of the (001)[110] partial fibre component and about 30% of two symmetrical components (111)[ $\bar{1}\bar{1}\bar{2}$ ] and (111)[112].

Note that the analytical form of the ODF allows to construct any PF {hkl}.

Thus in describing component composition of real textures it seems reasonable besides an indication of the crystallographic directions (hkl)[uvw] of a component coinciding with the rolling plane and the rolling direction, respectively, to specify also the texture axis direction of the component in the form (hkl)[uvw]| $\Psi_0, \theta_0, \phi_0$ |. Indices  $lu'v'w'$  and angles  $|\Psi_0, \theta_0, \phi_0|$  are related by :

$$\begin{aligned} \cos \theta_0 &= \frac{w'}{\sqrt{(u')^2 + (v')^2 + (w')^2}} , \\ \sin \phi_0 \sin \theta_0 &= \frac{u'}{\sqrt{(u')^2 + (v')^2 + (w')^2}} . \end{aligned} \quad (18)$$

The  $\Psi_0$  value may be selected arbitrarily since a change of this angle results only in a rotation of the coordinate system of a component texture axis around the texture axis (Oz-axis) and plays no part in the formation of the crystallite spread itself (see Figure 1.e-h). The  $\Psi_0$  value will effect values of the  $\Psi_1, \theta_1, \phi_1$  angles which rotate the already formed distribution of crystallites into the final one described by the orientation (hkl)[uvw]| $lu'v'w'$ |.

To conclude, it should be pointed out that the suggested model provides a common principle of simulation for the entire PF spectrum from single crystals at  $\sigma_1, \sigma_2, \sigma_3 \rightarrow 0$  to an isotropic polycrystals at  $\sigma_1, \sigma_2, \sigma_3 \rightarrow \infty$ .

## References

1. H. J. Bunge, *Mathematische Methoden der Texturanalyse*, Akademie-Verlag, Berlin (1969).
2. J. Hirsch and K. Lücke, *Acta Metall.*, **36**, 2863 (1988).
3. J. Jura, *Bull. Polish Acad. of Sci.*, **36**, 183 (1988).
4. K. Lücke, J. Pospiech, K. H. Virnich, and J. Jura, *Acta Metal.*, **29**, 167 (1981).
5. S. Matthies, *Phys. Stat. Sol. (b)*, **112**, 705 (1982).
6. R. J. Roe, *J. Appl. Phys.*, **36**, 2024 (1965).
7. T. I. Savelova, *Zavodskay labor.*, **50**, 5, 48 (1984).
8. D. Schläfer and H. J. Bunge, *Texture*, **1**, 157 (1974).
9. G. Wassermann and J. Grewen, *Texturen Metallischer Werkstoffe*, Springer-Verlag, Berlin (1962).